



HAL
open science

Evolution of physico-chemical and mechanical properties of bonded epoxy assemblies during hygrothermal cyclic aging

Hassan Obeid, Steven Marguet, Bouchra Hassoune-Rhabbour, Tiphaine Mérian, Aurélie Léonardi, Jean-François Ferrero, Héléne Weleman

► To cite this version:

Hassan Obeid, Steven Marguet, Bouchra Hassoune-Rhabbour, Tiphaine Mérian, Aurélie Léonardi, et al.. Evolution of physico-chemical and mechanical properties of bonded epoxy assemblies during hygrothermal cyclic aging. *Mechanics & Industry*, 2023, 24, pp.40. 10.1051/meca/2023036 . hal-04413258

HAL Id: hal-04413258

<https://hal.science/hal-04413258>

Submitted on 7 May 2024

HAL is a multi-disciplinary open access archive for the deposit and dissemination of scientific research documents, whether they are published or not. The documents may come from teaching and research institutions in France or abroad, or from public or private research centers.

L'archive ouverte pluridisciplinaire **HAL**, est destinée au dépôt et à la diffusion de documents scientifiques de niveau recherche, publiés ou non, émanant des établissements d'enseignement et de recherche français ou étrangers, des laboratoires publics ou privés.

History of matter: from its raw state to its end of life
Prof. Amine Ammar (Guest Editor)

REGULAR ARTICLE

OPEN ACCESS

Evolution of physico-chemical and mechanical properties of bonded epoxy assemblies during hygrothermal cyclic aging

Hassan Obeid^{1,2}, Steven Marguet², Bouchra Hassoune-Rhabbour¹, Tiphaine Mérian¹, Aurélie Léonardi³, Jean-François Ferrero¹, and Héléne Weleman^{1,*}

¹ Laboratoire Génie de Production (LGP), INP-ENIT, 47 avenue d'Azereix, 65016 Tarbes, France

² Institut Clément Ader (ICA), Université de Toulouse, CNRS UMR 5312, UPS, INSA, ISAE-SUPAERO, IMT Mines Albi, 3 rue Caroline Aigle, 31400 Toulouse, France

³ CLIX Industries, 2-3 allée de Longuetterre, 31850 Montrabé, France

Received: 22 December 2022 / Accepted: 10 October 2023

Abstract. This work investigates the hygrothermal cyclic aging of epoxy-based bonded assemblies. The focus is given here to severe long-term environmental conditions. The aging procedure is performed between 70° C with a relative humidity of 90% and -40° C without humidity, over a cyclic period of 12 h and for a total exposure time of 2 months. The aim of this study is to highlight the consequences of such hygrothermal aging on physico-chemical and mechanical parameters at both the material scale (adhesive) and the structural scale (bonded assemblies). Evolution of water absorption and glass transition temperature with aging cycles are monitored on adhesive bulk specimens by gravimetric analysis and DSC analysis respectively. The evolution of the quasi-static mechanical behavior, strength and elongation at failure, is characterized on adhesive massive specimens and on Single Lap Joint assemblies. Results show a progressive and important degradation of physico-chemical and mechanical properties with the number of cycles, of greater amount than that observed during static aging (loss of SLJ strength by 30% after 56 aging days; loss of the adhesive T_g by 45% for around 5% water uptake after aging 21 days). This behavior is related with an embrittling effect at the adhesive scale very specific to water change of state involved in these aging conditions. This combined analysis at different scales ensures a deep understanding of physico-chemical phenomena induced by hygrothermal aging and provides significant information for the further modeling of bonded joints assemblies.

Keywords: bonded assemblies; cyclic hygrothermal aging; severe environmental conditions; lap joint; mechanical testing; physico-chemical characterization

1 Introduction

Among the technical solutions that can reduce the weight of mechanical systems, structural bonding appears as a relevant alternative for the assembly of materials. The possibility of associating materials of different nature and properties, the preservation of the assembled parts and the quasi-continuous diffusion of the efforts between the elements are as many assets for this process and explain its rise in several fields of engineering. For automotive industry, the use of bonded assemblies typically offers a promising way to reduce the vehicles weight, and thus to decrease the CO₂ emissions and energy consumption. The success of structural bonding depends both on the performance of the adhesive itself and on the suitability of the adhesive with the parts being bonded. Epoxy-based polymer adhesives are specially designed for

structural bonding due to their high stiffness and strength properties associated with customized formulation able to match different kind of supports and various service requirements.

In several applications, bonded structures are exposed to severe environmental conditions where humidity and temperature may significantly affect the mechanical performance of adhesive joints. Many researchers have highlighted the effects of this aging on epoxy joints [1–3]. The water absorption generally leads to plasticity and/or breakage of interfacial bonds. At first, water molecules occupy the free volume of microcavities of the polymer. Then, water molecules penetrate the polymer network and break the weak bonds between the polar groups, reducing the glass transition temperature T_g of the adhesive and its mechanical properties, this phenomenon is called plasticization [4]. This water penetration directly results in a dimensional change of the polymer, known as swelling [5]. Generally, both plasticization and swelling are reversible.

* e-mail: Helene.Weleman@enit.fr

Yet, under certain conditions and for long time aging, differential deformation caused by water absorption can lead to microcracking and hydrolysis that correspond to the breakage of the polymer molecular chains [6]. Such irreversible damage induces a permanent degradation of the physico-chemical and mechanical properties of the adhesive and strongly reduces its lifetime [7,8]. In the works of Zhang et al. [9], the gravimetric monitoring of epoxy adhesives immersed in water at room temperature during 30 days shows a correlated kinetics between T_g reduction and water uptake in the first days of exposure then followed by some stabilisation of T_g while absorption still goes on. This is a direct consequence of the plasticization and bonding by type I bound water. Additionally, the partial recovery of the T_g after re-drying of saturated samples demonstrates the irreversible character of the water absorption. These changes are naturally reflected in the adhesive mechanical behavior. For instance, Mishra and Singh [10] have observed the degradation of the tensile strength according to exposure time for an epoxy-hardener system immersed in deionized water for 75 days at 20°C (see also [11,12]). Using FTIR analyses, they confirm the occurrence of hydrolysis phenomena that create carboxylic acids (C=O) and alcohol (OH). In addition to the negative impact of water on the adhesive material itself, the diffusion of critical amount of moisture at the interface with adherends may also lead to interfacial failure, the amplitude of this phenomenon being conditioned by the surface treatment [13,14]. The resulting consequence of these phenomena at the structural scale has been highlighted for example by Hirulkar et al. [15] on Single Lap Joints prepared with Aluminium substrates and Araldite[®] adhesives. They note a decrease by almost 25% of the shear strength after immersion in water during 60 days.

The above degradation processes due to humidity are generally strongly influenced by the temperature. Especially, high temperature may accelerate and increase previous modifications in physico-chemical and mechanical properties. Typically, the rate of sample weight gain and equilibrium level are higher for the high temperature immersion in [9]. Such observation is in line with the results of Zhou and Lucas [16] on three epoxy systems immersed at 60°C and 90°C during 65 days. For high temperature, the depression kinetics of the glass transition temperature is faster but with less amplitude than for low temperatures exposition. In their case, T_g begins to recover gradually with time after saturation. This is explained by the subsequent increase in type II bonds, which promote secondary crosslinking with hydrophilic groups such as hydroxyls and amines in the epoxy network. Precisely, higher immersion temperature induces a greater degree of T_g recovery. Xu et al. [17] have also demonstrated the irreversible changes occurred in a DGEBA epoxy subjected to long-term hygrothermal aging (immersion in deionized water at 75°C during 105 days). After re-drying of saturated samples, they note only a partial recovery of the T_g and mechanical properties (in tension, compression and shear strength). FTIR analyses confirm the chemical change affecting C-H bonds and intermolecular hydrogen bonds as in [16] and the faster

initiation of hydrolysis as in [10]. Regarding mechanical properties, the comparison of hygrothermal aging at 20°C, 50°C and 75°C by [10] shows that adhesive materials subjected to the highest hygrothermal aging temperature have the lowest value of tensile strength. Observation of such tendency is also extrapolated at the structural scale on SLJ specimens by [15] (see also [12]).

Despite an extensive literature on the question of hygrothermal aging of adhesives and bonded joints, the environmental conditions really encountered during vehicle service are often partially accounted. A first point stands in the consideration of cold temperature involving a change of water state. To our knowledge, one can only cite the study of Hu et al. [18] on SLJ specimens bonded with different adhesives and subjected to room temperature, 80°C and -30°C with 10–20% relative humidity for 7 days. Whatever the adhesive, the most severe and fastest degradation of SLJ strength is observed at -30°C, which demonstrates the weakening effect of negative temperatures turning the adhesive glass-like and increasing internal stresses. Another important fact is that bonded structures often undergo cyclic aging due to variational environmental conditions. Most studies, and in particular those cited above, only consider static aging conditions with fixed humidity level and fixed temperature. The response of the adhesive to cyclic aging is still relatively unexplored and existing studies generally consider few number of cycles or low impact conditions. The aging cycle applied by Moazzami et al. [19] on an Araldite[®] adhesive consisted of three runs with 100% relative humidity followed by one desorption phase each. They observe that the elastic modulus and tensile strength of the material decrease with increasing number of aging cycles together with an increase of the water content. Considering four cycles at 50°C including each a 30 days immersion period followed by a 7 days drying period, da Costa et al. [20] highlight that the water uptake and diffusion coefficient are mainly modified after the first cycle, the behaviour of the adhesive remaining quite constant for following cycles. Hirulkar et al. [15] investigated the effect of cyclic hygrothermal aging composed of two 6 h blocks involving different temperatures (between 50°C and room temperature; between 50°C and -5°C, without water phase change) and different environments (water and air) for each block. The breaking strength and maximum elongation of single-layer assemblies with either ductile or brittle Araldite[®] decrease significantly with the number of cycles. At last, the hygrothermal aging cycle used by Hu et al. [21] from 80°C to -30°C with 2 h period, constant humidity (10–20%) and during 14 days leads to a fast degradation of SLJ strength in the initial cycles, which then stabilizes at a loss of around 5% until the end of the test. Yet, according to short time exposure to each temperature, these conditions may not involve the complete phase change of moisture diffused within the adhesive joint.

This paper intends to investigate the hygrothermal aging behavior of assemblies bonded with an epoxy adhesive currently used in transport applications (Permabond Loctite[®] ESP 110). The main contribution of the present experimental study stands in the severe

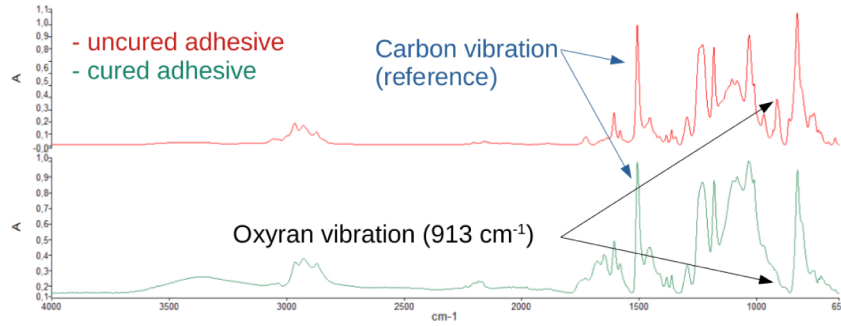


Fig. 1. FTIR spectrum for uncured and cured ESP 110 adhesives.

environmental conditions applied for hygrothermal aging. Cyclic, extreme and long-term conditions are considered, including an important number of variations from high to cold temperatures and from high to low humidity levels. Exposure times to each state are also sufficiently long to involve several water change of state between liquid to solid. Moreover, the understanding and characterization of such degradation mechanism requires studies at both the adhesive material and assembly structural scales. In this way, it is proposed to monitor the water uptake, the glass transition temperature, the bulk adhesive mechanical behavior and the resulting mechanical behavior of bonded assemblies (Single Lap Joint configurations). If damage effects on SLJ assemblies exhibit some similarities with those observed during static hygrothermal aging, we note in this case a specific behavior of the adhesive material that becomes much more brittle and an accelerated degradation kinetics of both physico-chemical properties and mechanical properties with aging cycles.

2 Materials and methods

2.1 Epoxy-based adhesive

The adhesive considered in this study is a standard brittle epoxy adhesive Permabond Loctite[®] ESP 110 reinforced with 30% aluminum powder filler and 5% of rubber to increase the modulus and ultimate strength of the adhesive [22]. The supplier recommends to cure the adhesive at 180°C within 20 min. Such protocol was checked by Fourier Transform InfraRed (FTIR) spectroscopy. Using Beer Lambert's law (1), which establishes a proportionality between the concentration of a chemical entity and its absorbance, the comparison of oxyran cycles (vibration band at 913 cm⁻¹) and carbon bonds (reference stretching vibration band at 1507 cm⁻¹, Fig. 1) makes it possible to determine the curing ratio c_r :

$$c_r (\%) = 100 \times \left(1 - \frac{\frac{H(913 \text{ cm}^{-1})_t}{H(1507 \text{ cm}^{-1})_t}}{\frac{H(913 \text{ cm}^{-1})_{t=0}}{H(1507 \text{ cm}^{-1})_{t=0}}} \right) \quad (1)$$

where $H(x)$ corresponds to the absorbance of the chemical entity with the wavelength x . After several tests, the

curing time was doubled to 40 min which ensures a value of $c_r = 96\%$ for the curing ratio.

Another important feature is the glass transition temperature T_g of the adhesive, which is the signature of the material. Indeed, an optimal T_g is a synonym for a maximal cross-linked density of the polymer. It was obtained by Differential Scanning Calorimetry (DSC), which consists of measuring the temperatures and heat flows associated with transitions in the material as a function of time and temperature in a controlled atmosphere. It was measured using a TA Instruments Q100 DSC machine. A temperature range of 20°C to 140°C was used in this experiment, with a heating rate of 5°C/min. The midpoint technique is used to calculate the T_g (Fig. 2). Precisely, the glass temperature of the cured adhesive was evaluated to 102°C ± 3°C, which stands in agreement with the supplier data.

2.2 Manufacture of SLJ and bulk specimens

The single lap joint specimens were prepared according to the French standard NF EN 1465 (Fig. 3). The adherent material used is Stainless Steel 304L for its resistant properties against corrosion. An overlap length of 25 mm × 12.5 mm was considered and a thickness of 0.4 mm was targeted thanks to a system of compression and Teflon wedges (Fig. 3b). A precise procedure was defined and used throughout all the production to ensure the same qualities on all specimens. For the surface preparation, the adherent was grit blasted using aluminum oxide particles. Substrates were then cleaned with pressurized air before degreasing them using alcohol in an ultrasonic tank for 10 min. The adhesive was then applied on the substrate using a 3D printed syringe with a rectangular slot. This method ensures a full application of the adhesive on the whole overlap area while reducing porosity (Fig. 4). The other substrate was finally laid down by tilting it to repel air bubbles and minimize trapped bubbles. After curing time, assemblies were left in the oven until it reached the room temperature. Thickness of the final adhesive bond was controlled by a calliper. An average value of 0.37 mm was obtained without significant dispersion along the overlap length nor between samples (standard deviation of 0.04 mm). Before any aging or testing, all specimens were stored in a desiccator.

In order to investigate the correlation between the macro and the micro scales behavior, the physico-chemical

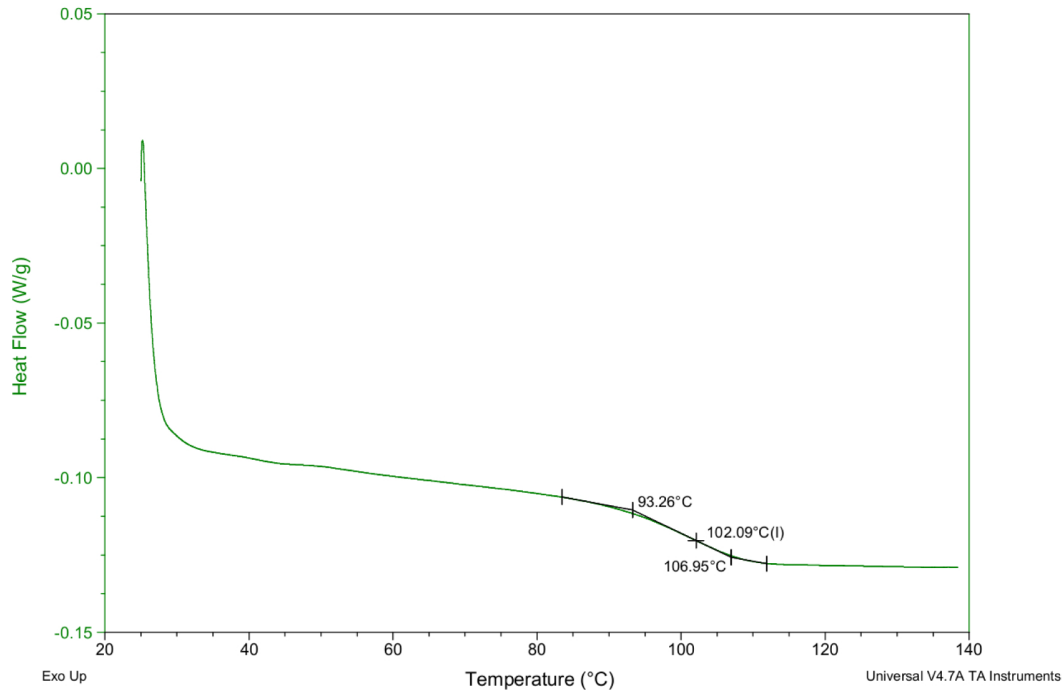


Fig. 2. Determination of the glass transition temperature T_g for ESP 110 by DSC.

and mechanical properties of the adhesive itself must be characterized. In this way, several types of specimens are required. A rectangular (40 mm × 10 mm × 42 mm) sample is used to measure the diffusion of water and the evolution of the T_g . For the tensile tests, dumbbell-shaped specimens were used (Fig. 5), inspired by the EN ISO 527-2 standard modified by Costa et al [11] to produce more reliable results.

To manufacture the bulk specimens while ensuring a good quality of samples, the NF T 76-142 standard was used, which consists on making first an adhesive plate of the desired thickness. The protocol is as follows: the adequate quantity of adhesive is poured on a Teflon plate which serves as a protection for the hot press and also ensures a smooth surface for the adhesive plates. This quantity is placed into the center of a rectangular silicone frame with a 2 mm thickness and an interior dimension of 145 mm × 145 mm, an outer metal frame is then placed around the silicone frame to maintain it in place during the manufacturing (Fig. 6a). Then another Teflon plate is placed on the top to hold the silicone frame in place while pressing (2 MPa). After the curing cycle, the plates are then cut using the water jet machine to obtain the final specimen geometries (Fig. 6b). As for assemblies, samples are then stored in the desiccator until aging and testing steps.

2.3 Aging conditions and gravimetric monitoring

Hygrothermal aging of all specimens has been carried out in an Excal 4021-T/H climatic chamber following the cycle d4 of the laboratory aging conditions for testing bonded joints defined by ISO 9142 standard [23] (Fig. 7). Cycle d4 trusts aging procedure used in the industry on bonded

assemblies as it simulates environmental conditions that vehicles can be exposed to during their life cycle. Each cycle lasts 12 h and consists of two phases:

- A first step of 5 h where the temperature is maintained at 70°C under a 90% relative humidity,
- A second one of same duration at −40°C and without any humidity.

Characterizations were thus planned in the initial state ($t_0 = 0$ day) and after 1 day (2 cycles), 2 days, 3 days, 7 days, 14 days, 21 days, 28 days, 42 days, 56 days (2 months, 112 cycles) of aging. Indeed, special attention is given here to short term effects that are often of most importance in adhesive materials aging. For each sampling, 3 specimens were considered for material and assemblies characterizations, which typically led to a total of 30 dumbbell-shaped adhesive specimens and 30 SLJ specimens. After each extraction, samples were placed within the desiccator at room temperature for 72 h prior to the experimental tests to allow stabilization.

After each extraction, the weight was measured to track the amount of water uptake. The specimens were taken out of the climatic room and wiped clean with Joseph paper sheets before being weighed using a high precision laboratory balance (accuracy of 0.01 mg). The water uptake M_t was calculated as $M_t = (w_t - w_0) / w_0$ (expressed in %), where w_t is the mass of the sample at the time t of extraction and w_0 the initial mass at $t_0 = 0$ day.

2.4 Mechanical testing

The adhesive strength of the single-lap shear joints was carried out on an Instron 100 kN hydraulic machine at

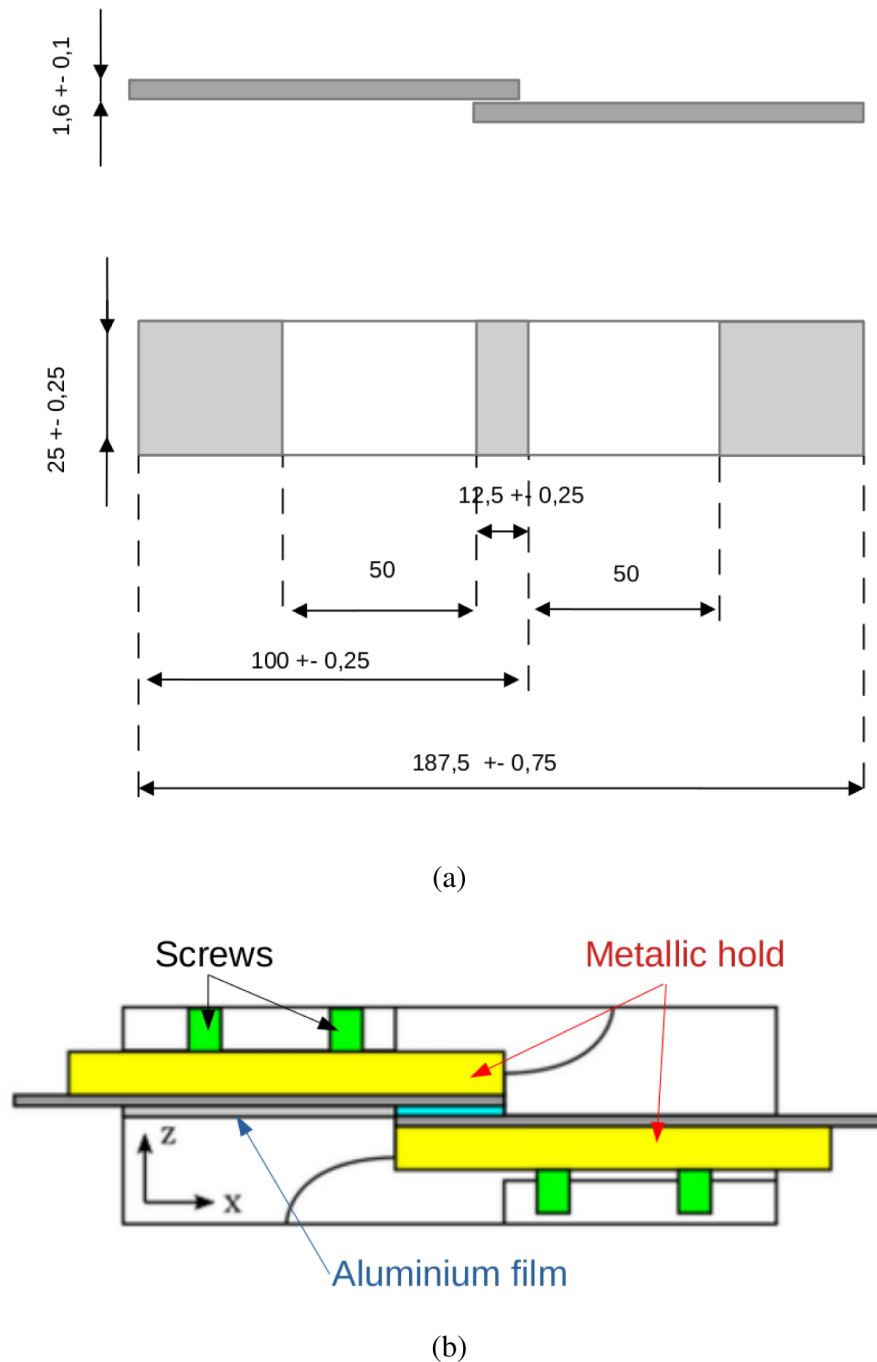


Fig. 3. (a) SLJ geometry according to NF EN 1465, (b) device used for the manufacture of assemblies.

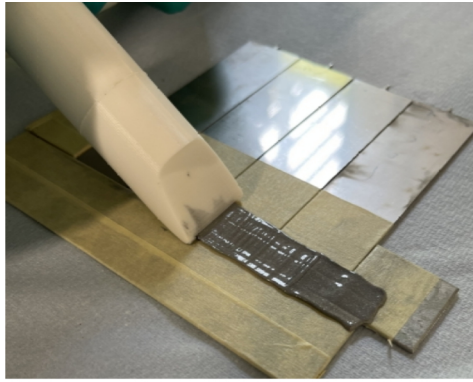
a constant displacement rate of 1 mm/min. Force values were provided by the Instron machine, while displacement values were determined using a digital image correlation technique (Fig. 8a). For each extraction, the mean values (failure force and maximum elongation) were averaged from tests performed on 3 specimens.

For tensile tests on bulk material, the alignment of the specimen and machine jaws requires special attention to avoid parasitic bending moments during testing. In this way, a special device was created to properly position the specimens and their holding fixations (Fig. 8b). Tensile

tests were then performed under constant displacement rate of 1 mm/min on an Instron machine with a 10 kN load cell. Similar monitoring procedure as for SLJ is considered (Fig. 8c).

3 Results and discussions

Figure 9 shows the force displacement curves of both SLJ assemblies and bulk adhesive before aging ($t_0 = 0$ day). Results for the 3 specimens considered in each



(a)



(b)

Fig. 4. (a) Application of the adhesive, (b) manufactured assemblies.

configuration are presented. Both [Figures 9a](#) and [9b](#) highlight the repeatability of the response, which confirms the reliability of manufacturing protocols. For assemblies and adhesive, the curves present first a linear part then followed by some non-linear transition up to failure. It shows that the elastoplastic behavior of the adhesive governs the assembly response with higher rigidity induced by metallic adherends in the case of SLJ samples (initial rigidity of 23.7 kN/mm for SLJ and of 616 N/mm for bulk specimens).

[Figure 10](#) shows the force displacement curves of both SLJ assemblies and bulk adhesive up to 56 days of aging. Among 3 tests done for each extraction time, the represented curve corresponds to the intermediate failure strength obtained; error bars on the top of the curve shows extreme values (low and high) obtained for the 2 other non-represented specimens. Note that the average relative deviation on all data between the average breaking force on 3 curves and the breaking force of the selected curve is around 6% for the bulk material and 8.5% for SLJ assemblies. Such dispersion stands in agreement with results obtained in the literature on similar test configurations and either for static or cyclic aging (see for instance [\[10,21\]](#)). Regarding the SLJ specimens ([Fig. 10a](#)), their behavior remains brittle throughout the aging process. In the first exposure times (up to 14 days), the response is quite homogeneous with small instabilities. For longer aging, the response comes to be more brittle

(similarly to [\[15\]](#)), with a global decrease of the stiffness and maximum load. At 56 days, we observe a plateau in the load-displacement response that may correspond to a plasticization of the adhesive joint. As in works of [Sugiman et al. \[24\]](#) for an immersion in deionized water at 50°C, the degradation of assemblies strength (around 30% at 56 days) is greater than the stiffness one (less than 5% at same time). It is worth noting that for a shorter time of severe cyclic aging, the magnitude of strength loss here is greater than the long-term static aging studied by these authors (24% after 2 years). Sub-zero temperatures undoubtedly play an important role in this degradation, in line with the higher level of SLJ strength degradation obtained in static aging conditions at -30°C than at 80°C in the comparative analysis of [Hu et al. \[18\]](#). Related failure facies of assemblies are presented on [Figure 11](#) for several aging times. The failure appears to be cohesive near substrate. An adhesive layer still remains on each side of the tested specimen, which means that the defined protocols ensures good initial conditions for the samples before testing them. Moreover, it is also important to note that the manufacturing procedure and the adhesive properties make it possible to preserve a cohesive failure mode under extreme aging conditions at least for 2 months. Even if the global behavior of assemblies is degraded with aging, the load transfer and the interface still hold within such structural bonding. Due to the viscosity of ESP 110, the presence of some bubbles inside the adhesive could not be completely avoided (for instance, third facies of [Figure 11f](#) for 56 aging days). While the presence of bubbles can weaken the adhesive joint, they do not appear to initiate cracks. In fact, fracture facies with bubbles present the same typology as the others, and do not systematically lead to significant dispersion in mechanical response (see related dispersion behavior for 56 aging days on [Figure 10a](#)).

Focusing now on the quantitative effects of hygrothermal aging, [Figure 12a](#) represents the evolution of the SLJ failure load versus aging time. Standard deviation is represented for each serie. In the same spirit, the evolution of failure displacement is described on [Figure 12b](#). These graphs show the progressive reduction of the mechanical properties of assemblies due to aging. Basically, the aging behavior can be separated in several phases. During the first 2 weeks, we observe a transitional phase with ups and downs for both failure force and failure displacement. The maximum load drops by 10% in the first 2 days of aging before recovering back in the 3rd day. Then, failure force values decrease again strongly after 2 weeks, up to 25% from $t = 0$ day. For 2 months of aging (56 days), one gets around 70% of the initial failure load but the dropping rate tends to be lower than in the early days. The trend on failure displacement is also a global reduction with aging but the standard deviations are too large to observe such detailed developments. This overall decrease of mechanical features seems to be due to a weakening of the adhesive joint mechanical properties induced by the water uptake. When water diffuses in the adhesive, it first occupies the free volumes and then starts breaking the weak bonds. This has for main consequence the global reduction of the maximum loading. Water can also locally

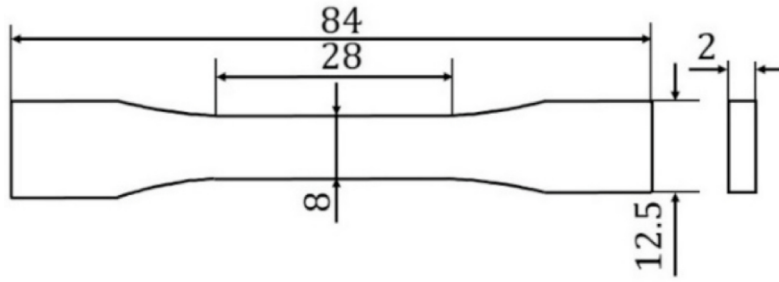


Fig. 5. Dumbbell-shaped geometry (in mm) based on the EN ISO 527-2 and modified by Costa et al. [11].

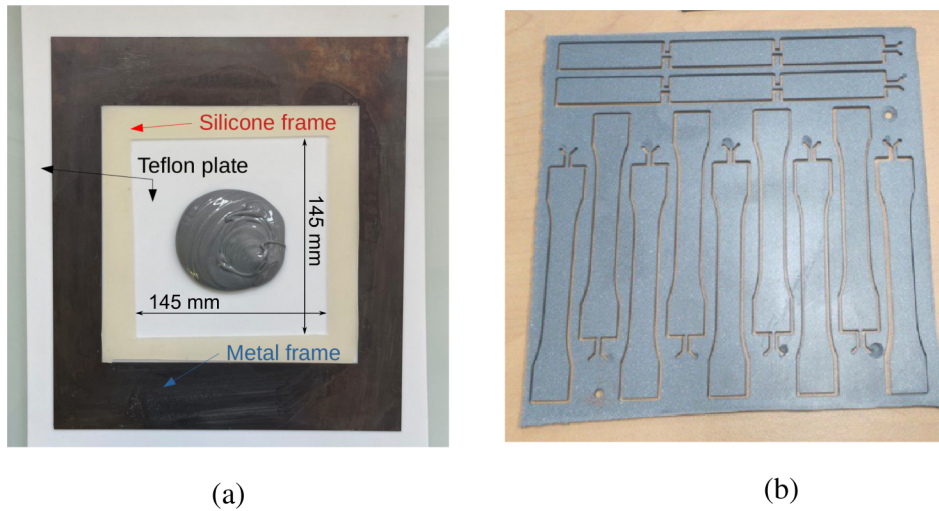


Fig. 6. Adhesive plate fabrication according to NF T 76-142: (a) pouring of the adhesive, (b) machined specimens.

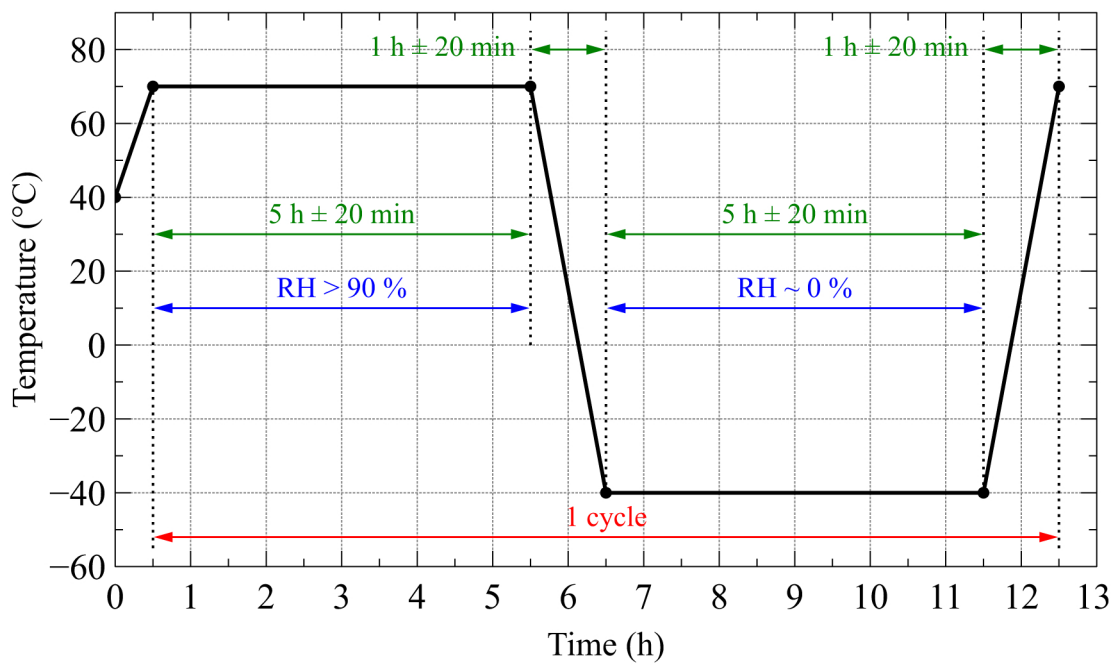


Fig. 7. Cyclic aging d4 according to ISO 9142 [23].

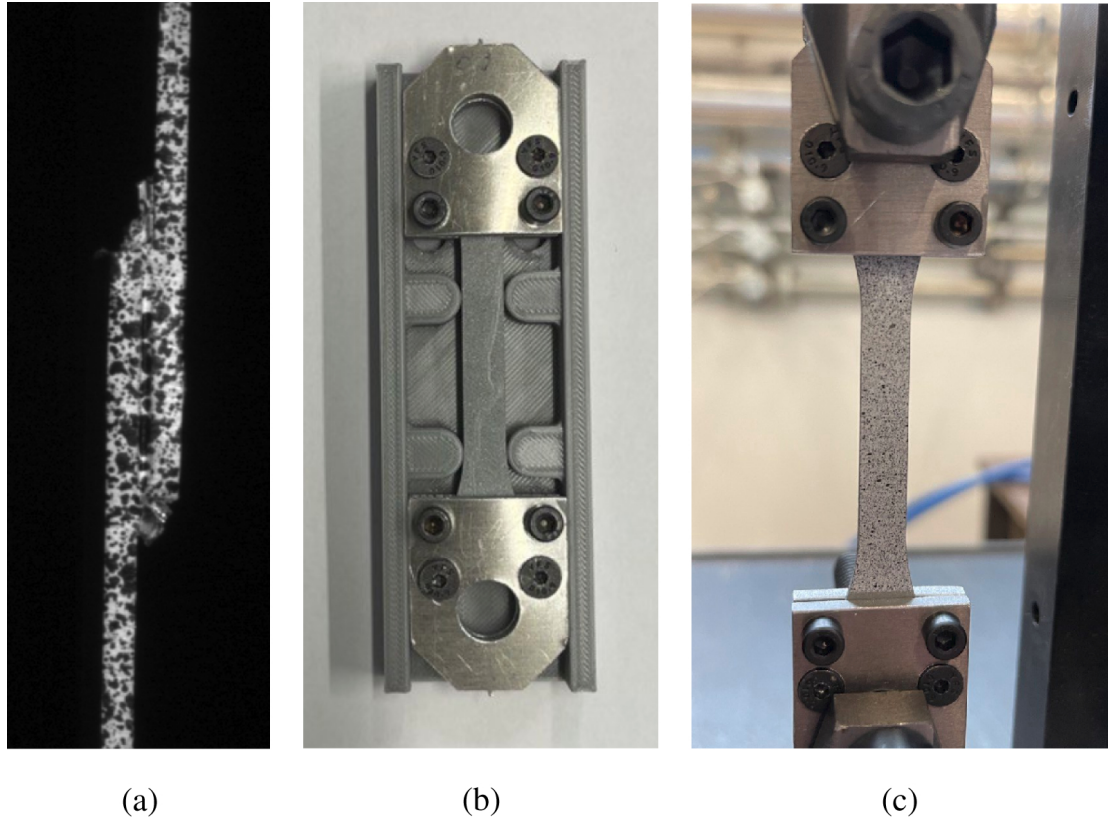


Fig. 8. Mechanical testing: (a) shear testing on SLJ assembly, (b) device for bulk specimen alignment, (c) tensile test on bulk adhesive.

form new bonds with the free molecules. This specificity of polymers may explain the small recovery in the failure loading observed at $t = 42$ days. Beyond that point, the influence of aging turns negative again for the failure strength adhesive, with much slower kinetics.

In order to better understand and explain the assemblies behavior, let us consider the response of bulk material. [Figure 13a](#) shows the water weight uptake as a function of the square root of time related to the thickness $h = 1.85$ mm of the sample. Up to 14 days ($\sqrt{t}/h \approx 600 \text{ s}^{1/2}/\text{mm}$), the diffusion is fast and linear, in agreement with a Fickian behavior. Then, it seems that there is a fall in the slope of the curve, corresponding to a decrease of the water uptake. Note that this latter point needs to be confirmed by additional long-term characterizations. After 21 days of aging, the weight gain reaches 4.4% while specimen are not saturated yet. Considering only earliest exposure times, one can estimate the diffusion coefficient D from classical linear part of Fick's law established for a thin adhesive submerged in an infinite bath:

$$\frac{M_t}{M_\infty} = \frac{4}{h} \sqrt{\frac{D t}{\pi}} \quad (2)$$

with M_∞ the mass of water intake at saturation. Following the same approach as [\[10\]](#), a short-time exposure diffusion coefficient has been estimated from the slope

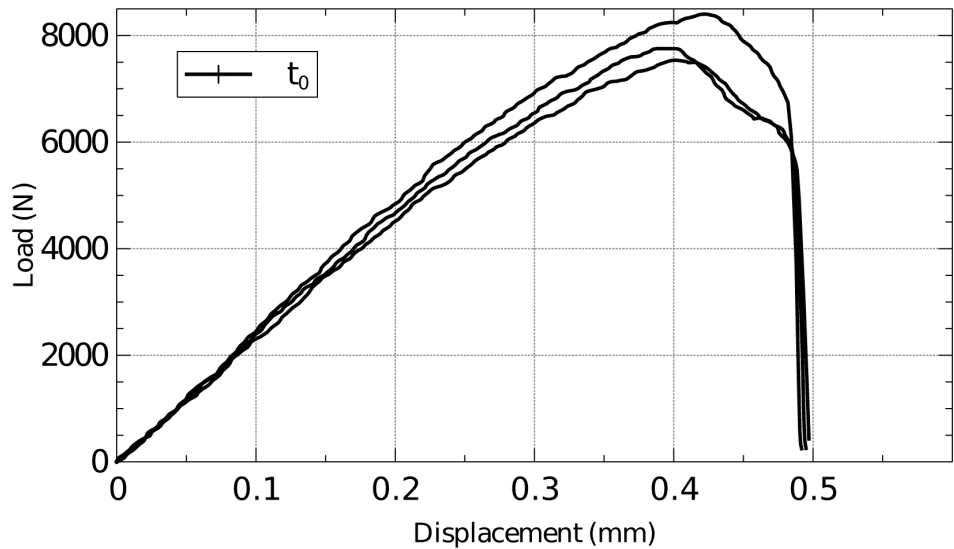
α of the straight (green) line in the pink region of the [Figure 13a](#):

$$D = \pi \left(\frac{\alpha}{4M_\infty} \right)^2 \quad (3)$$

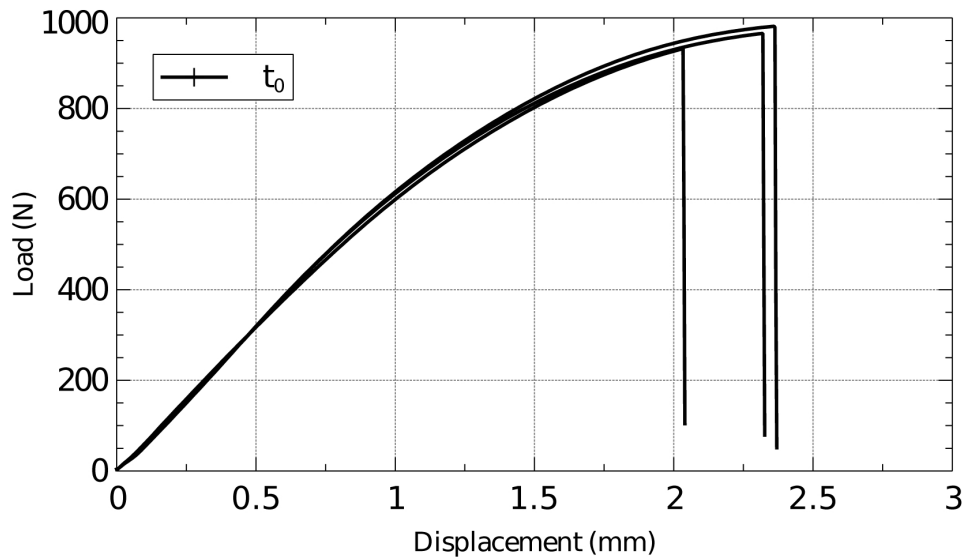
where the $M_\infty = 3.3\%$ has been taken at the point of linearity loss (red dotted line). It thus comes to $D = 9.69 \times 10^{-13} \text{ m}^2 \cdot \text{s}^{-1}$, which stands in agreement with usual results of the literature for epoxyde systems.

[Figure 10b](#) presents the evolution of the mechanical response of the bulk material. The curves show that the adhesive becomes even more brittle with aging time. Indeed, both the elongation and the breaking strength decrease during aging, as shown by [Figures 14a](#) and [14b](#). A drop by 40% for the failure load and by 50% for displacement at failure was observed through the first 7 days of aging. Beyond this, we note a stabilisation of the bulk mechanical response, both regarding failure force and displacement. Such embrittling effect is very specific to the present context since static aging at high temperature generally leads to a more ductile behavior of the adhesive related to water absorption [\[11,12\]](#).

During each aging cycle, the temperature variation induces a change of the absorbed water state from a liquid state to a solid state and vice versa. As the water diffuses, such recurrent state modification leads to a brittle behavior and thus a decrease of the T_g as illustrated



(a)



(b)

Fig. 9. Typical force displacement curves of mechanical testing before aging: (a) SLJ assemblies, (b) bulk specimens.

on Figure 13b. In the first 2 days, the T_g drastically decreases by almost 40% and reaches values around 65°C. From the 7th day, the T_g decreasing rate seems to lower (at $t = 7$ days, the T_g comes around 55°C), coming to some stabilization beyond that. Figure 13c makes it possible to estimate the relationships between the kinetics of water absorption and glass transition temperature evolution. One can observe in the first aging cycles a strong drop in T_g correlated with an important water gain (green dotted line interpolation). From the end of the linear Fickian behavior (14 days), it seems that there is some stabilization of the T_g degradation while absorption still goes on (red dotted line interpolation), as observed by [9] during static aging at room temperature. Note again

that this point needs to be confirmed by longer exposure cycles on the adhesive material. This overall drop of T_g causes the deterioration of the mechanical properties, as confirmed by the full correlation between the trend observed on the T_g and bulk mechanical properties evolution. More characterizations on the bulk material need to be made for longer times of aging to complete the understanding of the observed tendencies. Typically, it will be interesting to observe the kinetics of the water uptake to confirm if a first plateau has been reached between 7 and 14 days and whether the 42th day strength recovery on the SLJ assemblies actually corresponds to a material-wide strength recovery. Moreover, performing desorption at different aging times, typically after 7 days, could bring

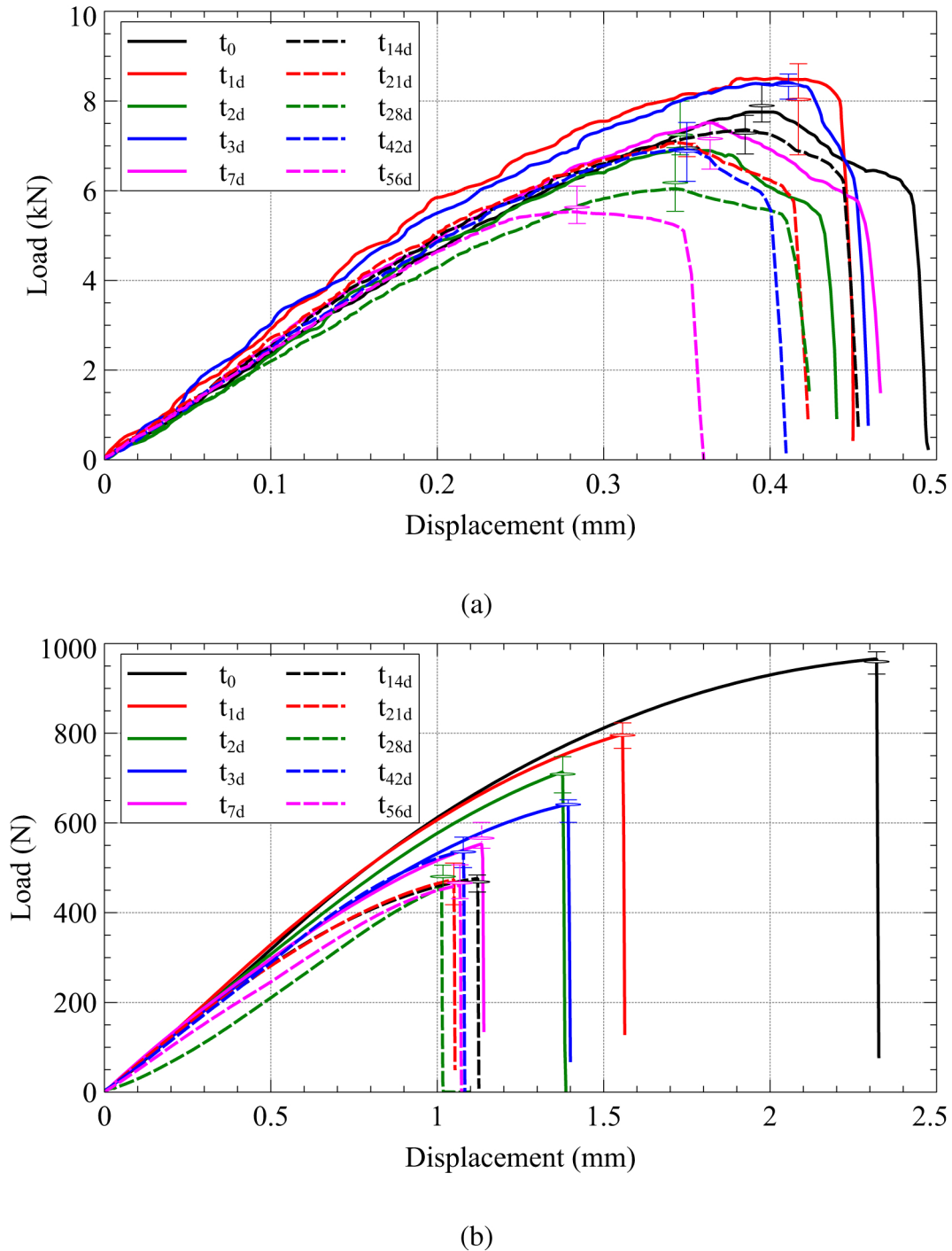


Fig. 10. Typical force displacement curves of mechanical testing for different aging times: (a) SLJ assemblies, (b) bulk specimens.

information on the reversible character of the adhesive degradation through the T_g recovery level.

4 Conclusions and perspectives

The influence of a cyclic hygrothermal aging on assemblies bonded with epoxy adhesive Permabond Loctite[®] ESP 110 was investigated in this study. Severe

long-term environmental conditions were considered, involving several water phase changes of state. Mechanical characterizations at the assembly scale (SLJ shear tests) and at the bulk material scale (tensile tests) were conducted, associated with physico-chemical analyses on the adhesive material. Throughout the aging process, the failure mode of SLJ remains cohesive while their behavior comes to be more brittle with a clear deterioration of their mechanical strength. First analyses on the

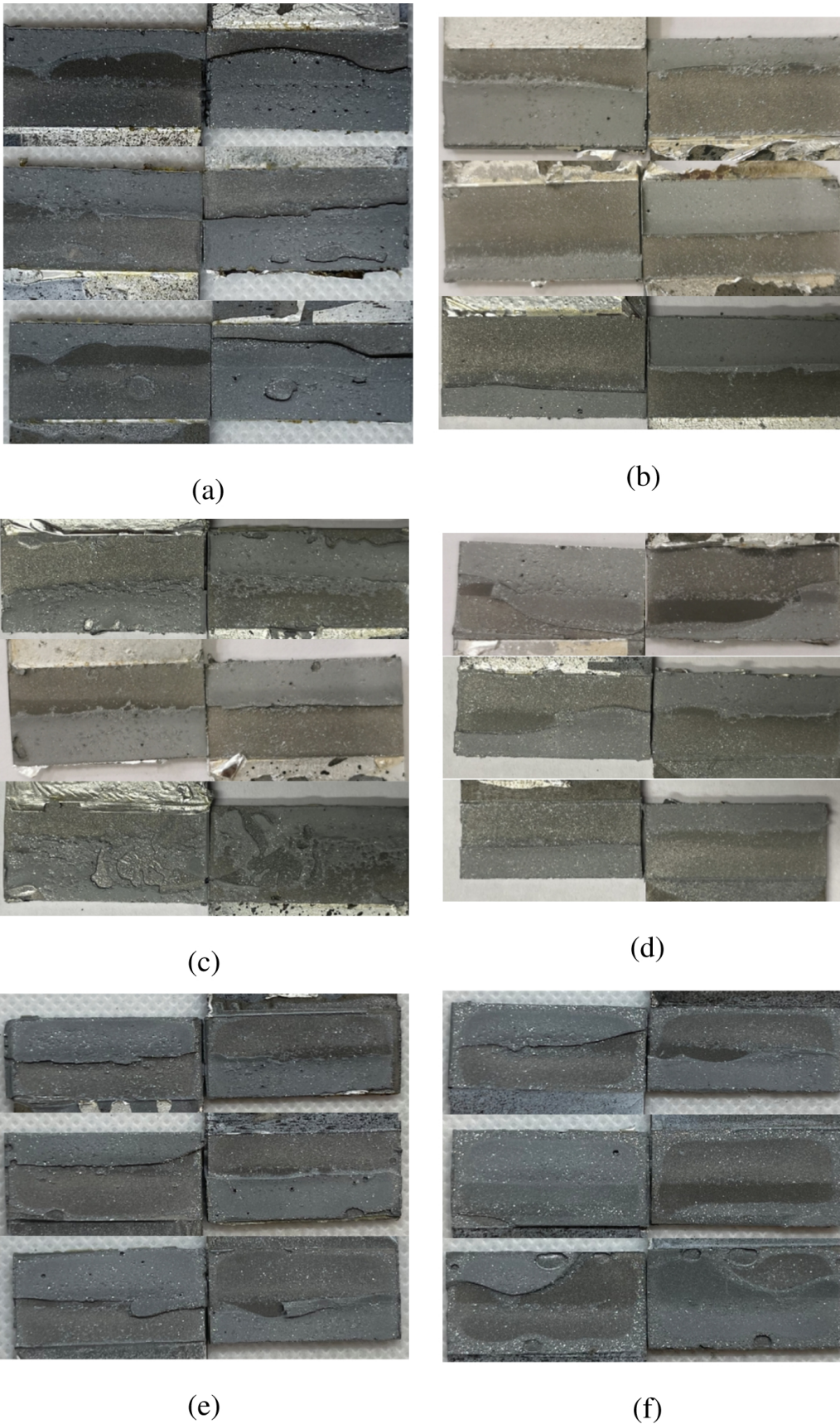


Fig. 11. Typical failure facies of SLJ assemblies for different aging times: (a) $t = 0$ day, (b) $t = 1$ day, (c) $t = 3$ days, (d) $t = 21$ days, (e) $t = 42$ days, (f) $t = 56$ days.

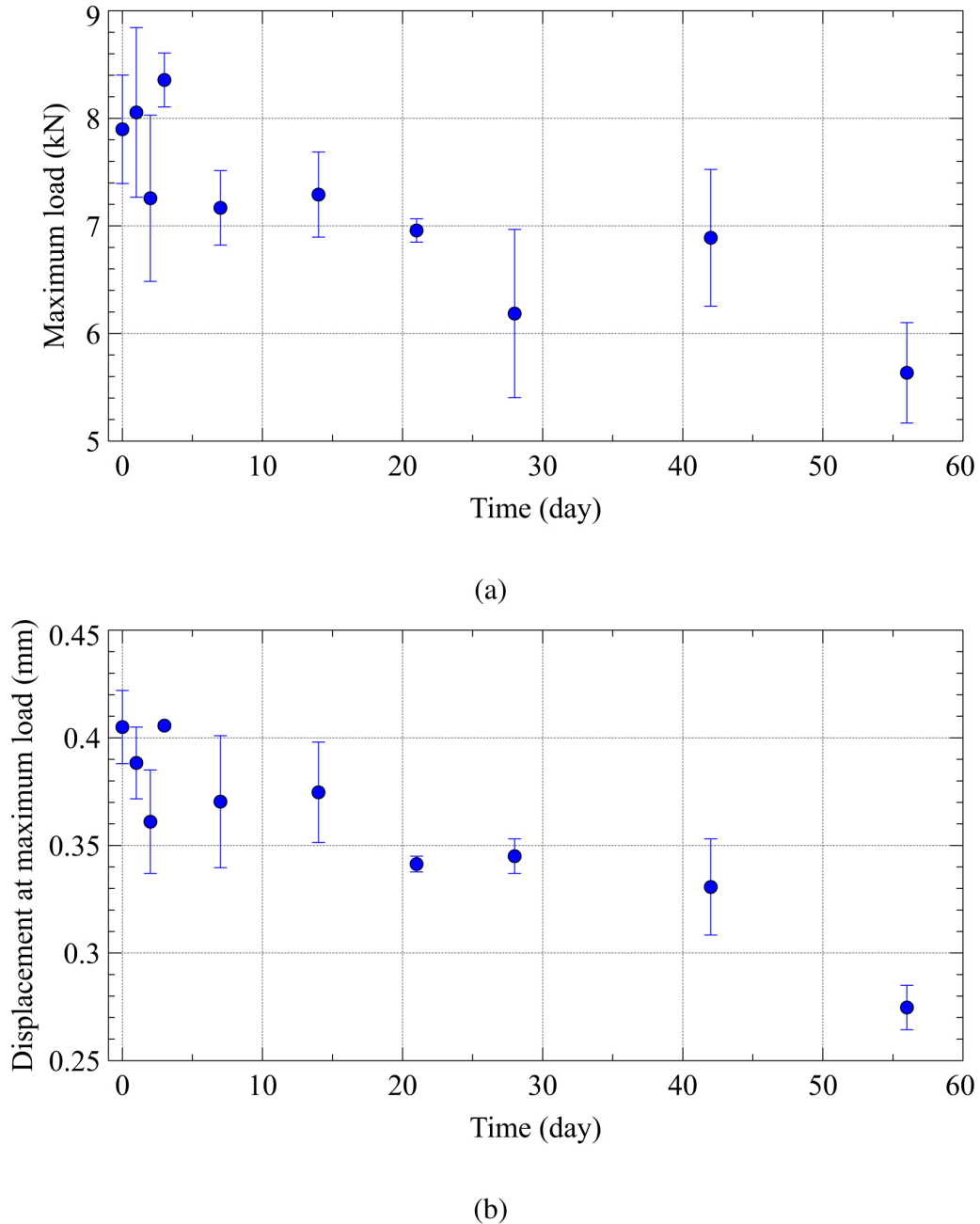
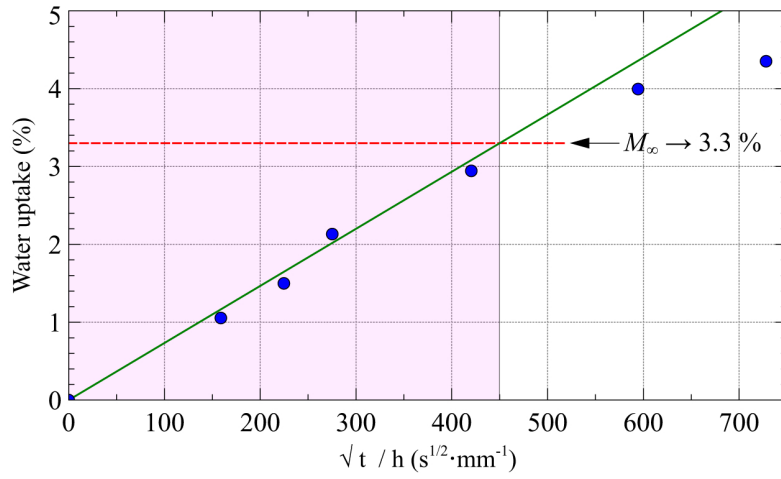


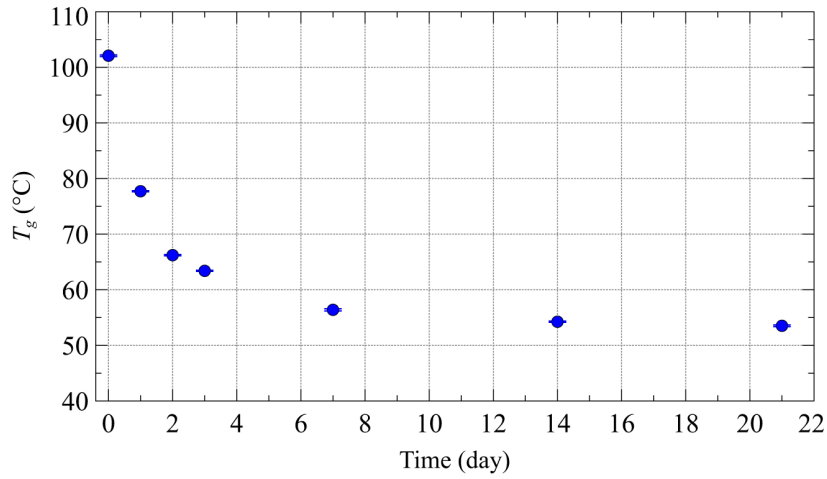
Fig. 12. SLJ shear test according to cyclic aging: (a) failure forces, (b) failure displacement.

evolution of physico-chemical and mechanical properties on the bulk adhesive show an important water uptake inside the adhesive related to a strong deterioration of its glass transition temperature. The water change of state during cyclic aging seems to explain the evolution towards a more brittle mechanical behavior of the adhesive very specific to present severe conditions, which would then be responsible for the damage observed in SLJ structures. Characterizations for longer aging times of bulk specimens could help understanding the

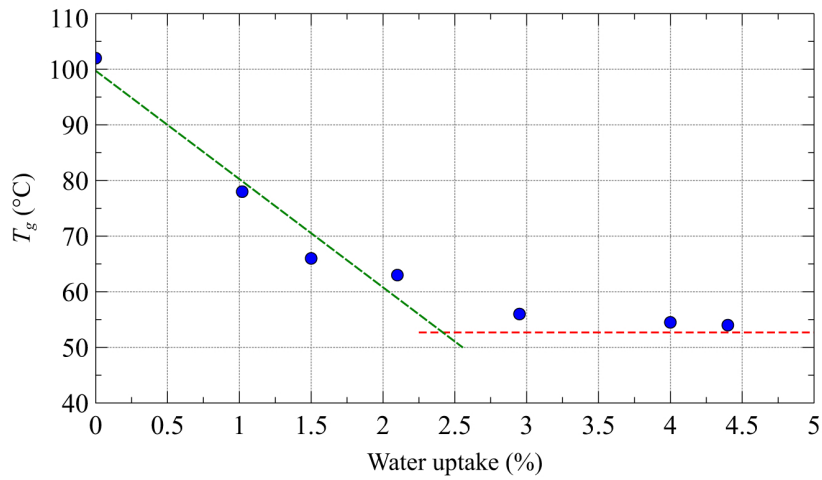
long-term behavior and specially the stabilization observed on assemblies. Other tests would provide also interesting information, such as FTIR analysis to investigate the evolution of the structural chemistry of the adhesive, desorption procedures and tensile tests with loading-unloading phases on aged bulk materials. This will provide crucial elements to identify physical and/or chemical damage phenomena induced within the adhesive, specially due to water phase changes involved under these severe conditions.



(a)

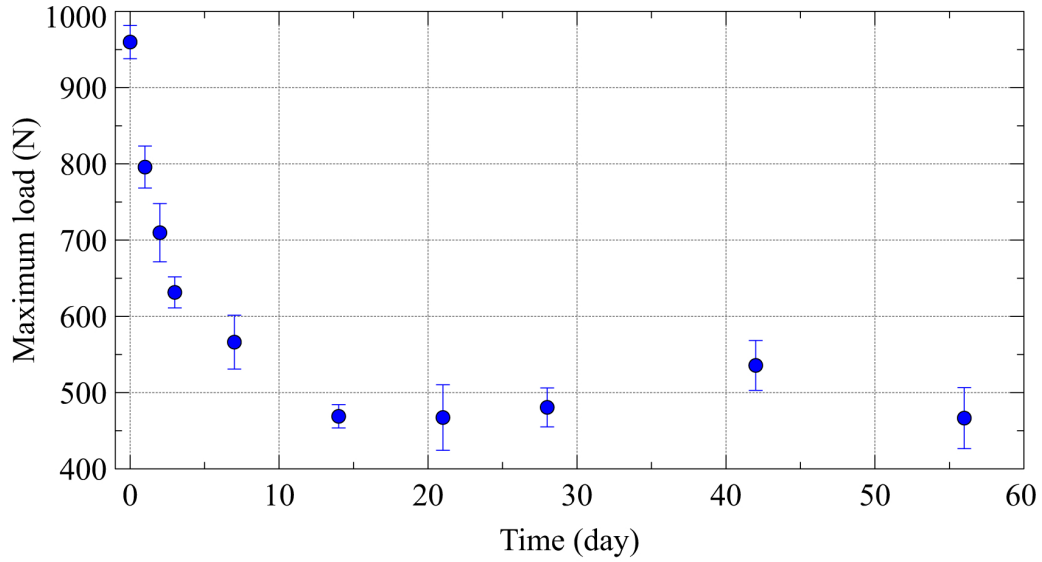


(b)

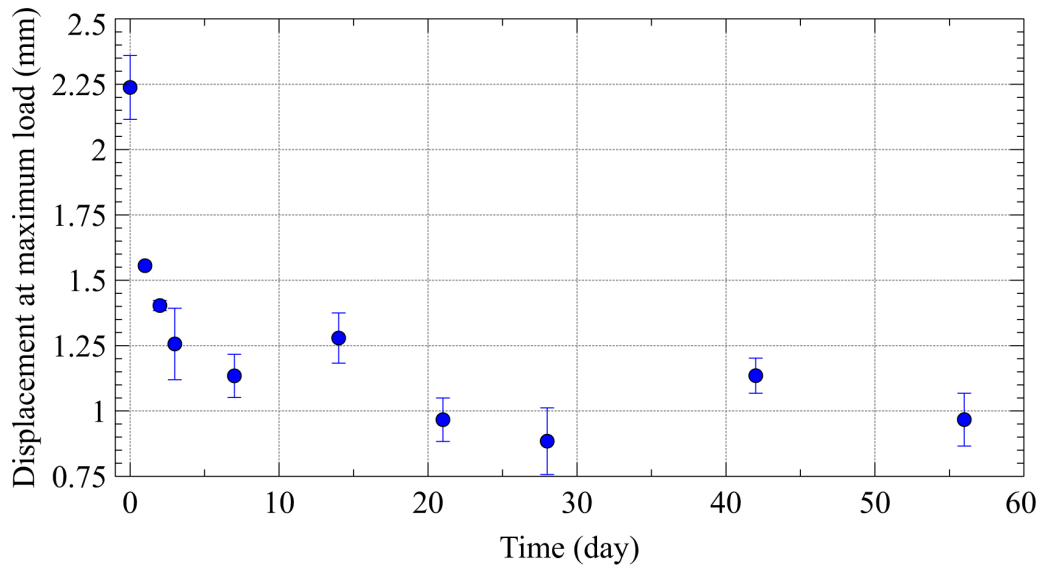


(c)

Fig. 13. ESP 110 mean physico-chemical parameters according to cyclic aging: (a) water uptake, (b) glass transition temperature T_g , (c) T_g versus water uptake.



(a)



(b)

Fig. 14. ESP 110 tensile test according to cyclic aging: (a) failure forces, (b) failure displacement.

Acknowledgement. Authors also thank the CLIX company for their scientific and financial support to the project.

Conflict of interest

Authors certify that they have no financial conflict of interest in connection with this article.

Funding

The Federal University of Toulouse Midi-Pyrénées (UFT-MiP) and the Urban Community of Tarbes Lourdes Pyrénées through INVICTUS project.

References

- [1] E.M. Petrie, Epoxy Adhesive Formulations – Epoxy Properties and Characteristics; Techniques for Improving Epoxy Strength, flexibility, and durability; testing and quality control guidelines, McGraw-Hill Chemical Engineering, New York, 2006
- [2] L. Grant, R.D. Adams, L.F. da Silva, Experimental and numerical analysis of single-lap joints for the automotive industry, Int. J. Adhesion Adhesives **29**, 405–413 (2009)
- [3] W. Possart, M. Brede, Adhesive Joints, Ageing and Durability of Epoxies and Polyurethanes, Wiley-VCH, Weinheim, 2019

- [4] L. Silva, S. Tognana, W. Salgueiro, Study of the water absorption and its influence on the Young's modulus in a commercial polyamide, *Polymer Test.* **32**, 158–164 (2013)
- [5] A. Toscano, G. Pitarresi, M. Scafidi, M. Di Filippo, G. Spadaro, S. Alessi, Water diffusion and swelling stresses in highly crosslinked epoxy matrices, *Polymer Degrad. Stabil.* **133**, 255–263 (2016)
- [6] G.L. de Oliveira, A.J.A. Gomez, M. Caire, M.A. Vaz, M.F. da Costa, Characterization of seawater and weather aged polyurethane elastomer for bend stiffeners, *Polymer Test.* **59**, 290–295 (2017)
- [7] L.F.M. da Silva, A. Ochsner, R. Adams, *Handbook of Adhesion Technology*, 2nd edn., Springer, 2018
- [8] X. Han, Y. Jin, W. Zhang, W. Hou, Y. Yu, Characterisation of moisture diffusion and strength degradation in an epoxy-based structural adhesive considering a post-curing process, *J. Adhesion Sci. Technol.* **32**, 1643–1657 (2018)
- [9] Y. Zhang, R.D. Adams, L.F.M. da Silva, Absorption and glass transition temperature of adhesives exposed to water and toluene, *Int. J. Adhesion Adhesives* **50**, 85–92 (2014)
- [10] K. Misra, A. Singh, Time-dependant degradation of highly cross-linked epoxy due to hygrothermal ageing at three different tem *Polymer Degrad. Stabil.* **215**, 110448 (2023)
- [11] M. Costa, G. Viana, C. Canto, L.F.M. da Silva, M.D. Banea, F. Chaves, R.D.S.G. Campilho, A.A. Fernandes, Effect of hygrothermal aging and cyclic thermal shocks on the mechanical performance of single-lap adhesive joints, *J. Mater. Des. Applic.* **230**, 968–982 (2016)
- [12] T.-C. Nguyen, Y. Bai, X.-L. Zhao, R. Al-Mahaidi, Durability of steel/CFRP double strap joints exposed to sea water, cyclic temperature and humidity, *Composite Struct.* **94**, 1834–1845 (2012)
- [13] D. Brewis, J. Comyn, R. Shalash, The effect of moisture and temperature on the properties of an epoxide-polyamide adhesive in relation to its performance in single lap joints, *Int. J. Adhesion Adhesives* **2**, 215–222 (1982)
- [14] J. Delozanne, N. Desgardin, M. Coulaud, N. Cu villier, E. Richaud, Failure of epoxies bonded assemblies: comparison of thermal and humid ageing, *J. Adhesion* **96**, 1–24 (2018)
- [15] N. Hirulkar, P. Jaiswal, P. Reis, J. Ferreira, Effect of hygrothermal aging and cyclic thermal shocks on the mechanical performance of single-lap adhesive joints, *Int. J. Adhesion Adhesives* **99**, 1025 (2020)
- [16] J. Zhou, J. Lucas, Hygrothermal effects of epoxy resin. Part II: variations of glass transition temperature, *Polymer* **40**, 5513–5522 (1998)
- [17] K. Xu, W. Chen, X. Zhu, L. Liu, Z. Zhao, G. Luo, Chemical, mechanical and morphological investigation on the hygrothermal aging mechanism of a toughened epoxy, *Polymer Test.* **110**, 107548 (2022)
- [18] P. Hu, X. Han, W.D. Li, L. Li, Q. Shao, Research on the static strength performance of adhesive single lap joints subjected to extreme temperature environment for automotive industry, *Int. J. Adhesion Adhesives* **41**, 119–126 (2013)
- [19] M. Moazzami, M. Ayatollahi, A. Akhavan-Safar, L.F.M. da Silva, Experimental and numerical analysis of cyclic aging in an epoxy-based adhesive, *Polymer Test.* **91**, 106789 (2020)
- [20] J.A. da Costa, A. Akhavan-Safar, E.A.S. Marques, R.J.C. Carbas, L.F.M. da Silva, Cyclic ageing of adhesive materials, *J. Adhesion* **98**, 1341–1357 (2022)
- [21] P. Hu, X. Han, L.F.M. da Silva, W.D. Li, Strength prediction of adhesively bonded joints under cyclic thermal loading using a cohesive zone model, *Int. J. Adhesion Adhesives* **41**, 6–15 (2013)
- [22] L.F.M. da Silva, R.D. Adams, The strength of adhesively bonded T-joints, *Int. J. Adhesion Adhesives* **22**, 311–315 (2002)
- [23] ISO 9142, Adhesives – guide to the selection of standard laboratory ageing conditions for testing bonded joints, *Int. Standard* (2003)
- [24] S. Sugiman, A.D. Crocombe, I.A. Aschroft, Experimental and numerical investigation of the static response of environmentally aged adhesively bonded joints, *Int. J. Adhesion Adhesives* **40**, 224–237 (2013)

Cite this article as: H. Obeid, S. Marguet, B. Hassoune-Rhabbour, T. Mérian, A. Léonardi, J.-F. Ferrero, H. Weleman, Evolution of physico-chemical and mechanical properties of bonded epoxy assemblies during hygrothermal cyclic aging, *Mechanics & Industry* **24**, 40 (2023)